Modification of Electrodes with Self-Assembled Hydrophobin Layers

Renata Bilewicz,*,† Jaroslaw Witomski,† Angeline Van der Heyden,‡ Denis Tagu,§ Béatrice Palin,§ and Ewa Rogalska*,‡

Department of Chemistry, University of Warsaw, ul. Pasteura 1, 02093 Warsaw, Poland, Equipe de Physico-chimie des Colloïdes, UMR 7565 CNRS/Université Henri Poincaré, Nancy I, Faculté des Sciences, BP 239, 54506 Vandoeuvre-lès-Nancy, Cedex, France, UMR IaM 1136 INRA/Université Henri Poincaré, INRA-Nancy, 54280 Champenoux, France

Received: April 12, 2001; In Final Form: June 19, 2001

The small fungal protein hydrophobin from *Pisolithus tinctorius* (HYDPt-1) has been used to modify electrode surfaces by self-assembly from aqueous solutions. Voltammetric experiments performed with $Fe(CN)_6^{3-}$ as an electrochemical probe have shown that hydrophobin can be immobilized on hydrophobic surfaces of a glassy carbon electrode (GCE), or on a thin mercury film electrode (TMFE), or on hydrophilic surfaces such as a gold electrode (GE). Higher efficiency of coverage is obtained for GCE or TMFE. The hydrophobin-modified electrodes were in turn functionalized with the electroactive ubiquinone (Q10), quinone (Q0), and azobenzene. While Q10 was adsorbed on the surface of the hydrophobin layer, smaller molecules, azobenzene and Q0, penetrated into the pores of the layer. In all cases, a stable attachment of the electroactive reagents to the electrode via the hydrophobin was achieved.

Introduction

Specific modification of surfaces is a major challenge in the engineering of function-oriented advanced materials. A frequently encountered bottleneck in micro-patterning and functionalization of surfaces is an absence of adequate methods for molecule immobilization. In the search for new methods of modifying electrode surfaces and for new modifying agents, numerous methods were elaborated, including coating with Nafion and other polymers, or self-assembly of thiol compounds.[1−5] In this work a small fungal protein, hydrophobin HYDPt-1, was used to modify different hydrophobic and hydrophilic electrode surfaces.

Hydrophobins[6−8] were first identified in the early 1990s and aroused much interest due to their unusual physicochemical properties,[9] their physiological role,[6,7,10] and potential medical and technical applications.[11] Hydrophobins are secreted by filamentous fungi,[6,11,12] the development of which depends on their capacity of adhesion[13] to different surfaces, and their growth through the air/water interface.[10] The interactions of the fungi with the environment are mediated by hydrophobins which aggregate at the fungal cell walls and other interfaces into amphipathic layers.[6] While no three-dimensional structure of any hydrophobin has been established until now, it is known that all hydrophobins described have a common structural feature of eight cysteine residues forming intramolecular disulfide bridges.[7,14−16] The hydrophobin isolated from *Schizophyllum commune* (SC3) is the most extensively studied. SC3 decreases the surface tension of pure water from 72 to 24 mN/m for a concentration of 0.05 mg/mL, and is the most surface-active protein known.[10,17] However, the hydrophobins are not surface active as monomers, and are therefore harmless to the cellular membranes of the producing fungus. Only after a structural rearrangement at the air/water interface do they self-assemble into a film and acquire their surface activity. SC3 and other hydrophobins assemble not only at the air/water interface[18] but also at water/hydrophobic fluid and water/solid interfaces.[10,11,13,19,20] Recent results obtained with atomic force microscopy indicate that *Agaricus bisporus* hydrophobin adsorbs to a hydrophobic surface of pyrolytic graphite from dilute solution to form a highly ordered monolayer with a rodlike pattern.[21] In the case of SC3 protein, the scanning force microscopy, infrared spectroscopy, and circular dichroism revealed that the monomeric, water-soluble form of the protein is rich in β-sheet structures and that the quantity of β-sheets increases after the adsorption of the protein at the air/water interface.[22] The formation of the β-sheets may be responsible for the decrease of the surface tension of water.[22] Adsorption of the protein to a hydrophobic solid surface induces specifically formation of an α-helix structure. The α-helix is rich in hydrophobic amino acids[22] and may act as an anchor that binds the protein to the surface, which phenomenon leads in turn to organization of the protein into amyloid-like rodlets.[9,22] The SC3 films formed via strong noncovalent interactions are highly insoluble and cannot be removed from hydrophobic surfaces even in hot sodium dodecylsulfate.[16]

In the present paper we describe the behavior of the hydrophobin from the fungus *Pisolithus tinctorius* (HYDPt-1) at the air/water and electrode/solution interfaces, and show that the protein layer may control the access of compounds from the solution to the electrode surface. Even more importantly, we show the ability of the hydrophobin to act either as a hosting matrix, or as a molecular glue binding electroactive molecules to the electrode. The effect of creating active centers in the otherwise nonelectroactive modifying layer is demonstrated, using azobenzene and quinone derivatives.

Experimental Section

Production and Purification of the Hydrophobin. HYDPt-1 hydrophobin was produced in *Escherichia coli* as a recombinant

* Author to whom correspondence should be addressed. E-mail: rogalska@lesoc.uhp-nancy.fr (or bilewicz@alfa.chem.uw.edu.pl).
† Department of Chemistry, University of Warsaw.
‡ Equipe de Physico-chimie des Colloïdes, UMR 7565 CNRS/Université Henri Poincaré, Nancy 1.
§ UMR IaM 1136 INRA/Université Henri Poincaré, INRA-Nancy.

10.1021/jp0113782 CCC: $20.00
Published on Web 08/07/2001

polypeptide of 13.7 kDa.[23] Briefly, the *hydPt-1* cDNA was cloned in the pQE30 plasmid (Qiagen, Germany) to produce a fusion protein with a His-tag motif. Extraction was performed as described previously.[23] After chromatographic purification on a Ni^{2+} affinity column, the HYDPt-1 polypeptide was concentrated in 10 mM Tris-HCl by ultrafiltration.

Chemicals and Solutions. All chemicals were of analytical grade. Tris(hydroxymethyl)aminomethane (Tris), dimethyloformamide (DMF), and LiOH were from Fluka. Coenzymes Q0 (2,3-dimethoxy-5-methyl-1,4-benzoquinone) and Q10 (ubiquinone 50) were from Sigma. Azobenzene was from Reachim, Hungary. Methanol, citric acid, and $K_3[Fe(CN)_6]$ were from POCh, Poland. All solutions were prepared daily. Distilled water was passed through a Milli-Q water purification system. The surface tension was 72.5 mN m^{-1} at 20 °C and final resistivity was 18.3 MΩ cm^{-1}.

Surface Pressure Measurements. Surface pressure measurements of hydrophobin solutions in water were carried out using KSV 5000 instrument (KSV, Finland). The software KSV-5000 was used to control the experiments. Kinetics of adsorption were measured for arbitrarily chosen concentrations of the protein, using 5 mL of freshly prepared solutions. The protein solutions were placed in a glass beaker covered with a tight-fitting cover, with a small opening for the stem of the Wilhelmy plate to go through. Covering the beakers was necessary to avoid water evaporation from the solutions; this precaution was particularly important in case of long-lasting measurements. Temperature was kept constant at 20 °C. The surface tension (γ)−log c dependencies were plotted using Π values obtained after the time needed for the solutions to attain the equilibrium.

Electrochemical Experiments. Voltammetry experiments were done at 20 °C in three-electrode arrangement, with a calomel reference electrode, platinum foil counter electrode, and GE, GCE, or TMFE as working electrodes. Eco Chemie AUTOLAB PGSTAT 30 system was used as the potentiostat with an IBM PC and Eco Chemie software. To prepare the TMFE, a silver wire or silver disk electrode, precleaned in concentrated perchloric acid, was touched to a drop of mercury and cathodically polarized in 0.1 M KOH to obtain a shining and uniform layer of mercury, ca. 1 mm thick. The GE and GCE were polished on Buehler polishing papers and paste, and the GE was then cleaned in concentrated nitric acid. The electrodes were coated with the self-assembled hydrophobin upon contact with the surface of solutions containing 2 μg of hydrophobin per 1 mL of 10 mM Tris-HCl buffer. The time of the hydrophobin self-assembly and the conditions of Q0, Q10, and azobenzene adsorption on hydrophobin-coated electrodes are given in the figure legends.

Results and Discussion

Formation of HYDPt-1 Films Adsorbed at the Air/Water Interface. To determine the surface properties of HYDPt-1, the surface pressure−time kinetics were recorded for the films adsorbed from bulk solutions to the air/water interface. Chosen examples of adsorption kinetics recorded for different bulk concentrations of HYDPt-1 (Figure 1) show that HYDPt-1 adsorption behavior is typical of water-soluble amphiphiles.[24] The time to reach the equilibrium and the time lag of surface pressure increase was longer for lower concentrations of the protein. The latter was as long as 90 min for the protein concentration of 0.2 μg/mL (Figure 1, curve 1), while for the concentration of 260 μg/mL (Figure 1, curve 4) it was nonmeasurably short. For the highest protein concentrations the initial increase of surface pressure was followed by its decrease

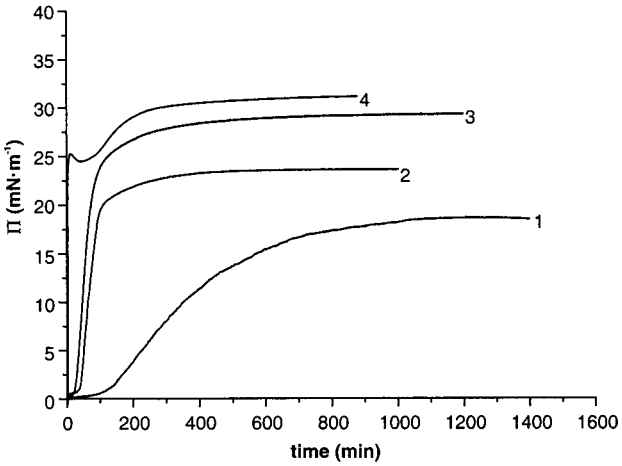

Figure 1. The surface pressure−time kinetics of HYDPt-1 adsorption to the air/water interface at 20 °C. Bulk concentration of HYDPt-1 was 0.2 μg/mL (curve 1), 2 μg/mL (curve 2), 25 μg/mL (curve 3), and 260 μg/mL (curve 4).

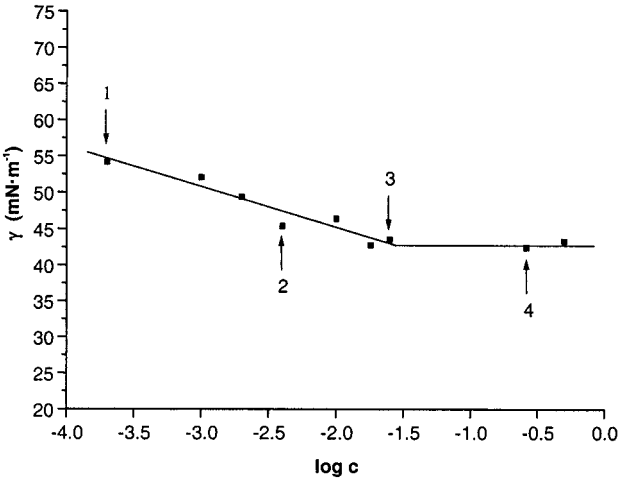

Figure 2. Surface tension vs log c curve for aqueous solutions of HYDPt-1. Symbols represent the measured values. The points indicated with arrows correspond to the curves shown in Figure 1.

and a further increase, reflecting a slow relaxation of a densely packed film. The surface pressure was systematically monitored as a function of time, to ensure that the calculated values of γ used to plot the γ−(log c) dependencies (Figure 2) corresponded to the thermodynamic equilibrium. Such was done by collecting the equilibrium surface pressure (Π) data for various bulk concentrations of the protein. Maximum surface excess concentration (Γ_{max}) and minimum area/molecule (A_{min}) at the air/water interface were calculated from relationships[25,26]

$$\Gamma = \frac{1}{2.303RT}\left(\frac{-\partial\gamma}{\partial \log c}\right)_T$$

$$A = 10^{14}/(N\Gamma)$$

where $(-d\gamma/d \log c)_T$ is the slope of the γ−log c plot at constant (absolute) temperature, T, R = 8.314 J mol^{-1} K^{-1}, and N is Avogadro's number. The calculation of Γ_{max} gave a value of 9.91×10^{-11} mol cm^{-2} and, correspondingly, the A_{min} value of 167 Å^2. Assuming a spherical shape, this protein of 13.7 kDa would have a calculated diameter of approximately 32 Å and the cross-section of 804 Å^2. In the absence of any three-dimensional structure of hydrophobin, and based on the comparison of the experimental value of the molecular area and

the theoretical cross-section, we hypothesize that in the conditions of saturation of the interface with the protein, the HYDPt-1 has an oblong form and that its long axis acquires a perpendicular orientation relative to the interface.

The HYDPt-1 lowered the surface tension of water at 20 °C from 72.5 mN/m to approximately 42 mN/m (Figure 2). It should be noticed here that the HYDPt-1 used in this study was produced in *E. coli* and at present we do not know, if its tertiary structure is identical with this of the protein produced by the fungus. Indeed, the value of the surface tension of HYDPt-1 water solutions, higher than this reported for the SC3[10,17] might be indicative of the absence or different formation of the four disulfide bridges. The latter problem will be addressed in our future studies using the native protein. Moreover, experiments performed with different batches of HYDPt-1 (results not shown) indicate that the surface activity of the protein depends significantly on the composition of different buffers used during the purification. The latter fact offers the possibility of optimization of the physicochemical properties of the protein for different applications; this point is presently under study in our laboratories.

Barrier Properties of HYDPt-1 Films on Gold and Glassy Carbon Electrodes. The properties of HYDPt-1 layers adsorbed on hydrophilic and hydrophobic solid surfaces were compared using three different electrode substrates, namely GE, GCE, and TMFE. The hydrophilic GE surface was modified with HYDPt-1 by self-assembling the protein at the liquid−air interface, followed by adsorption of the layer to the gold surface. The protein was assembled from 10 mM Tris-HCl buffer, pH 7.0, containing 2μg/mL hydrophobin, and adsorption to the surface was achieved by lifting the electrode up through the interface, or by a horizontal touching of the hydrophobin-covered water surface with the electrode. Figure 3 shows the cyclic voltammograms recorded using the bare and hydrophobin-modified electrodes. Figure 3a allows the comparison of the bare and covered GE. The curves are similar in that no decrease of background current is observed, and no peaks appear in the voltammogram. The presence of the hydrophobin layer on the electrode surface is evidenced by the inhibition of the final increase of anodic current due to gold oxidation. HYDPt-1 is inert in a wide range of potentials and does not lead to a decrease of capacity currents which means that the protein layers formed on the electrode are not as dense and highly blocking, as the layers of, for example, alkanethiols.[1] The extent of blocking is not changed even after 24 h of self-assembly.

Wessels and Wösten observed that the SC3 hydrophobin had much higher affinity to hydrophobic than to hydrophilic surfaces.[13,19] Two types of electrodes, GCE and TMFE, were therefore chosen as model hydrophobic surfaces to check the behavior of HYDPt-1. The results of self-assembly are shown in Figure 3b,c. In both cases the background currents become much smaller after modification, demonstrating that the coverage of GCE and TMFE with HYDPt-1 is much higher, compared to that of the gold substrate. The protein layers are stable and firmly attached to the electrode substrate, as indicated by the GCE voltammogram which does not change over several weeks. In the case of TMFE, high quality films are formed even when the time of self-assembly is decreased from 24 h to 20 min. The capacity of the modified TMFE is significantly lowered, and the onset of the mercury oxidation current is shifted toward more positive potentials, revealing good blocking properties of the hydrophobin layer. On the other hand, an additional peak appears in the TMFE voltammogram at −0.58 V. This peak corresponds to the reduction of mercury cysteinate formed on the electrode surface upon oxidation of mercury in the presence of cystein thiol groups present in the protein.

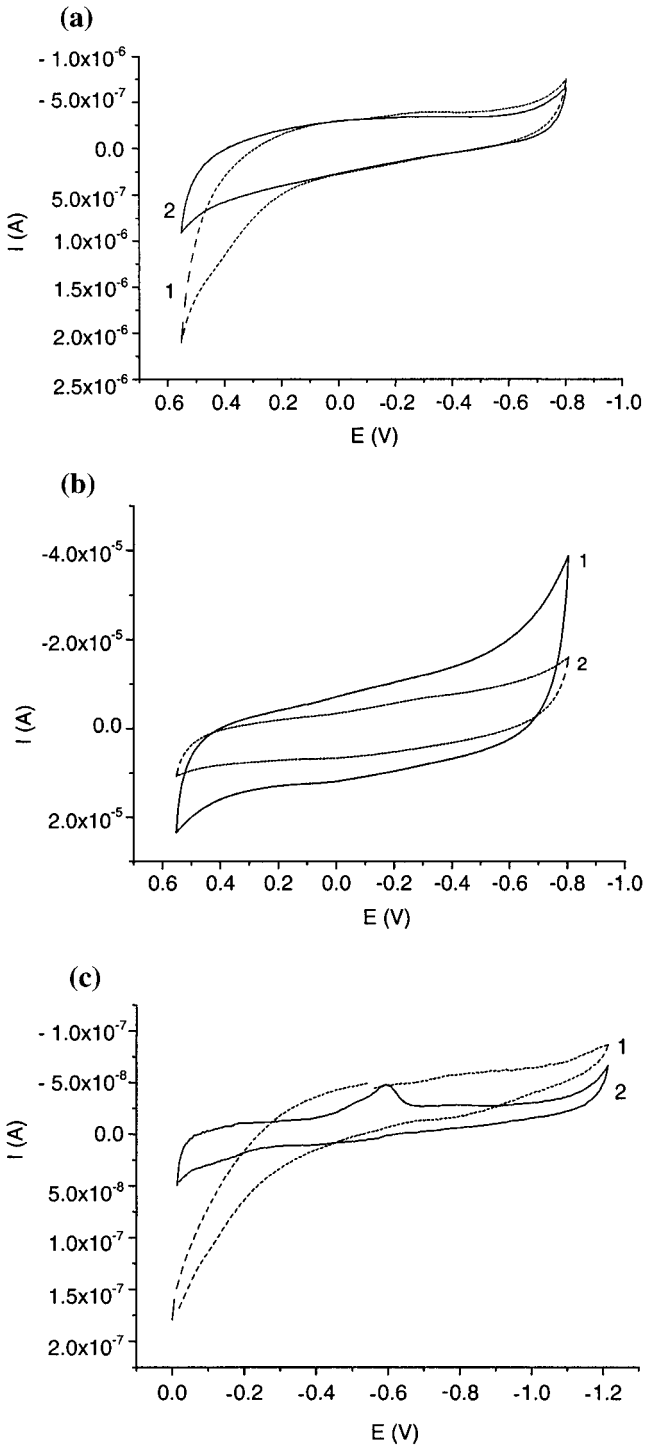

Figure 3. Cyclic voltammograms recorded in Tris 0.1 M/$HClO_4$ pH 7.0 on (a) GE, (b) GCE, and (c) TMFE (1) bare and (2) modified with HYDPt-1. Time of self-assembly: (a,b) 24 h, and (c) 20 min. Scan rate 0.1 V/s.

The oxidation of mercury in the presence of cysteine was studied by Bard and Stankovich who proposed the following scheme of the process:[27]

$$2(RSH) + Hg = [Hg(RS)_2]_{ads} + 2H^+ + 2e$$

The product of oxidation—ill-soluble $Hg(RS)_2$—remains adsorbed on the mercury surface. The voltammetric scan recorded on the bare and HYDPt-1 covered TMFE in a wide range of

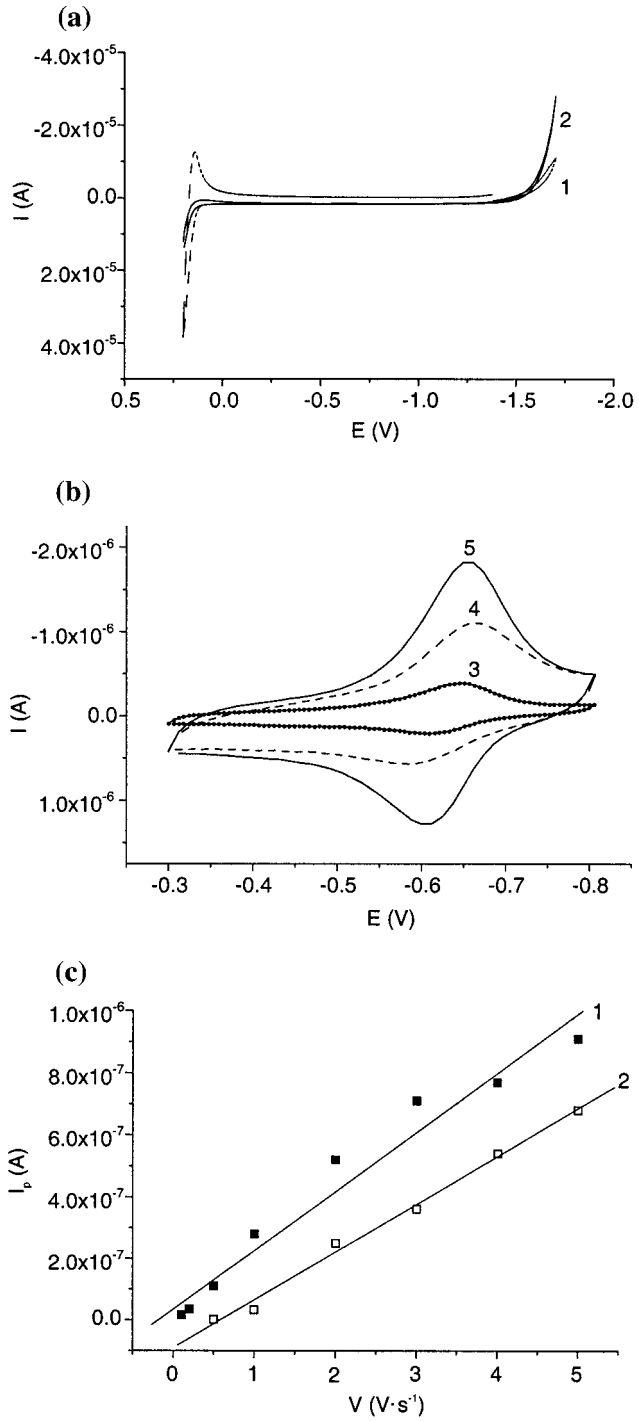

Figure 4. Cyclic voltammograms recorded in Tris 0.1 M/$HClO_4$ pH 7.0 on TMFE (1) bare and (2−5) modified with HYDPt-1. Time of self-assembly: 20 min. Scan rate: (1, 2) 0.1, (3) 1.0, (4) 3.0, (5) 5.0 V/s; (b) part of (a) enlarged to show the mercury cysteinate formation and reduction; (c) dependence of oxidation (curve 1) and reduction (curve 2) peak currents (I_p, absolute values) on the scan rate.

potentials are shown in Figure 4a. The scans indicate that the final oxidation of mercury is blocked in the presence of hydrophobin, as are also the reduction currents at positive potentials; however, the final reduction current corresponding to the reduction of hydrogen ions appears at less negative potentials. The voltammograms recorded at higher scan rates and narrower potential window (Figure 4b) exhibit the oxidation/reduction peaks connected with oxidation of mercury in the presence of thiol groups. The linear dependence of the peak current (I_p) on scan rate shown in Figure 4c confirms that both cysteines and the mercury compound are immobilized on the electrode surface.

The surface concentration Γ_c of cysteine groups may be calculated using the following equation: $\Gamma_c = Q/(nFA_e)$, where Q is the charge measured from the area under the reduction peak, n is the number of electrons exchanged, F is the Faraday constant (9.64867×10^4 C mol^{-1}), and A_e is the electrode area (0.02 cm^2). The average value obtained for Q from three independent experiments is 1.73×10^{-6} C cm^{-2}. Assuming that only one cysteine in each HYDPt-1 molecule is electroactive, the Γ_c and the surface concentration of HYDPt-1 (Γ_h) are 8.97×10^{-12} mol cm^{-2}, and the area occupied by one individual molecule of HYDPt-1 (A_h) on the electrode surface is 1853 Å^2. The Γ_h is approximately nine times lower than the HYDPt-1 concentration calculated at the air/water interface which gives, accordingly, higher values of molecular area for the HYDPt-1 adsorbed on the electrode. The latter differences would be even more pronounced, if more than one cystein in the HYDPt-1 was electroactive. The differences in surface concentration and molecular area at the air/water interface and electrode/solution may be indicative of different affinities of the HYDPt-1 for the two interfaces, and of a conformational rearrangement of the protein upon adsorption to the GE surface. Differences in surface coverage with HYDPt-1 were also observed in this work for the GCE, TMFE, and GE, and by Wösten et al. for the air/water and Teflon/water interface.[13,19] In both cases the higher coverage was observed with more hydrophobic surfaces.

Stability of HYDPt-1 Layers in Solutions of Different pH. The dependence of stability and blocking properties of HYDPt-1 layers on the pH of the solution was checked by recording multiple cyclic voltammograms using all electrodes in solutions of pH 2.2 (citric acid), pH 4.7 (citric acid/LiOH), pH 7.0, pH 10.2 (Tris), and pH 12.1 (LiOH). The HYDPt-1 layer remained well attached to the electrode surfaces in all solutions studied, and the blocking effect on various substrates followed the behavior observed at pH 7.0.

Probing Blocking Properties of HYDPt-1 Layers Using Ferrocyanate as the Electrochemical Probe. The ability of small hydrophilic anions to access the electrode surface through the HYDPt-1 layer was checked using ferrocyanate ions as the electrochemical probe. Cyclic voltammograms were recorded in 0.1 M/$HClO_4$ solution containing 0.75 mM $K_3Fe(CN)_6$ (Figure 5). The voltammograms recorded for $K_3Fe(CN)_6$ using HYDPt-1-coated electrodes are different, compared to those obtained with a bare GE or GCE. The currents are much lower and the voltammetric curves are more sigmoidal in shape. This behavior establishes that the extent of coverage of both electrodes by HYDPt-1 is high, and that the probe has a limited access to the electrode surface. The transition from peaked to sigmoidal shape is expected when the access sites are dispersed,[28,29] and when spherical diffusion becomes the major process for transporting the molecules to the electrode surface, as distinct from the linear diffusion observed for large bare electrodes.

The GCE surface is blocked more efficiently than the gold surface, as shown with the experiments performed in pure supporting electrolyte solution. The latter results confirm a higher affinity of HYDPt-1 toward hydrophobic surfaces.

Hydrophobin as a "Molecular Glue" for Immobilizing Molecules on the Electrode Surface. Wösten and de Vocht suggested that hydrophobin might be used to attach cells or molecules to hydrophobic surfaces in medical and sensing devices.[9] In the present work we checked the ability of HYDPt-1 to bind different types of electroactive molecules to electrode

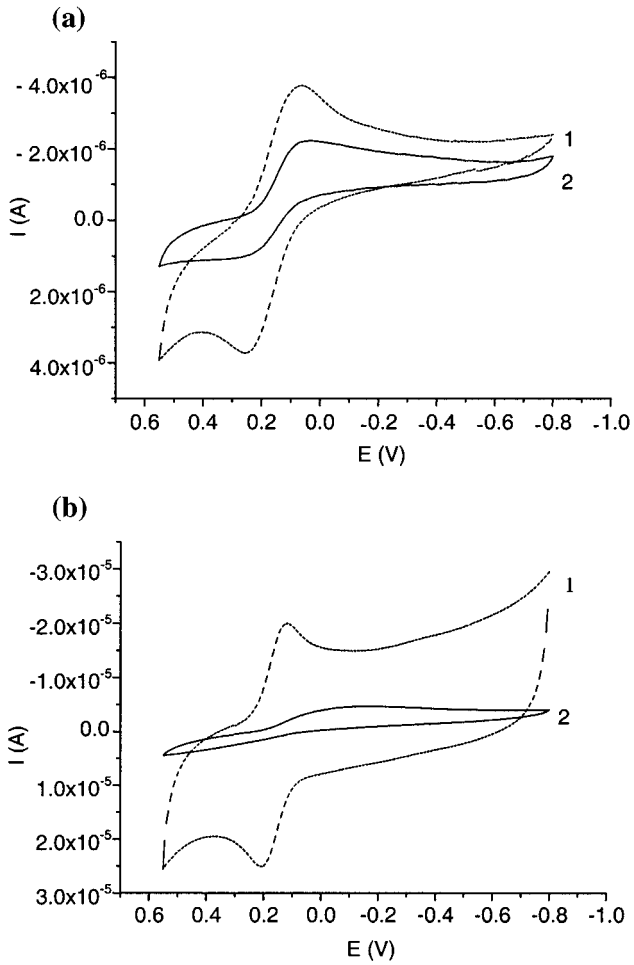

Figure 5. Cyclic voltammograms for 0.75 mM $K_3Fe(CN)_6$ in Tris 0.1 M/$HClO_4$ of pH 7.0 recorded on (1) bare and (2) covered with HYDPt-1 (a) GE and (b) GCE. Time of self-assembly: 24 h. Scan rate 0.1 V/s.

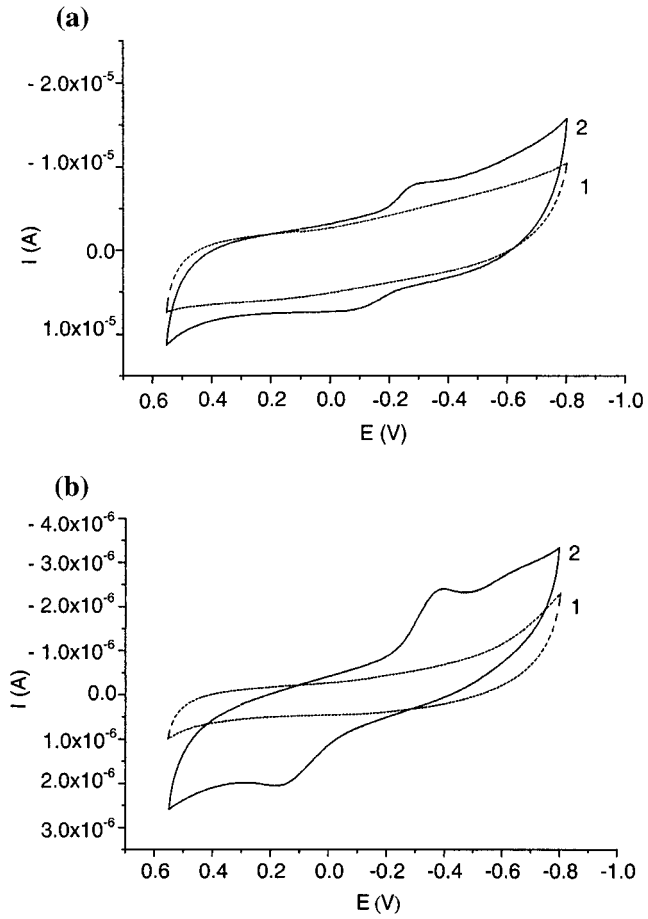

Figure 6. Cyclic voltammograms recorded in Tris 0.1 M/$HClO_4$ of pH 7.0, using GCE modified with HYDPt-1 layer (1) prior and (2) following the adsorption of Q10. Time of self-assembly in solution containing 1 mg Q10 /1 mL DMF: 30 min. Scan rate 0.1 V/s. (b) as (a) but using HYDPt-1 stored for 3 months at 4 °C.

SCHEME 1

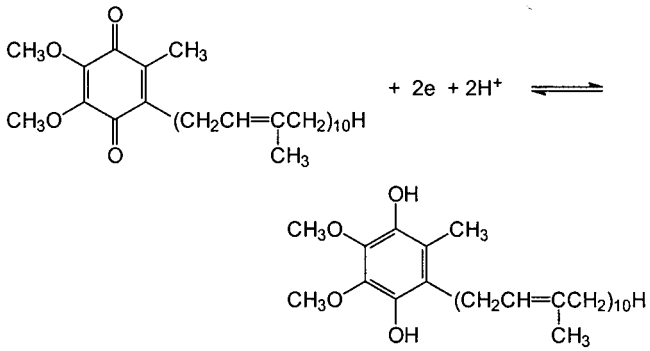

surfaces. The long hydrocarbon chain ubiquinone (Q10) was used as a model hydrophobic molecule. First, the HYDPt-1 layer was self-assembled on the GCE from the usual solution (2 μg/1 mL Tris buffer, pH 7.0). Next, self-assembly of Q10 was carried out from a solution containing 1 mg of Q10 in 1 mL of DMF.

Electroreduction of Ubiquinone Q10 Immobilized on Electrodes Modified with HYDPt-1. In neutral aqueous solution ubiquinone undergoes reduction, according to Scheme 1.[30] The voltammetric curve obtained with ubiquinone adsorbed on the HYDPt-1-modified GCE is shown in Figure 6. The shape of the curve and the linear dependence of the peak currents on the scan rate points to surface immobilization of ubiquinone. The GCE substrate covered with HYDPt-1 was found to bind

SCHEME 2

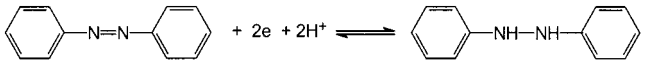

Q10 in a very stable way, giving rise to ubiquinone reduction and oxidation signals which remained unchanged for several weeks. When the adsorption of ubiquinone was carried out on the electrode coated with a HYDPt-1 stored for several months at 4 °C, less reversible systems of peaks were obtained (Figure 4b). In the latter case, the peaks of ubiquinone are even more visible and the background currents are smaller, but the separation of ubiquinone peaks is larger. This result indicates that the structure of HYDPt-1 underwent modifications, leading to a denser and barrier-like layer, more efficiently isolating the electroactive centers from the electrode.

Electroreduction of Azobenzene Immobilized on Electrodes Modified with HYDPt-1. Azobenzene is a small molecule with a photo- and electroactive azo group, which does not undergo adsorption on a bare glassy carbon electrode. However, when adsorbed on a HYDPt-1 modified electrode, azobenzene remains stably attached to the surface, even after repeated transfers of the electrode into solutions of different pH and not containing the azocompound. Self-assembly of azobenzene was carried out from a 1 mM methanol solution. Reduction of azobenzene can be described as shown in the Scheme 2.[31]

Figure 7 shows the cyclic voltammogram of azobenzene adsorbed for 20 min on the HYDPt-1-modified electrode,

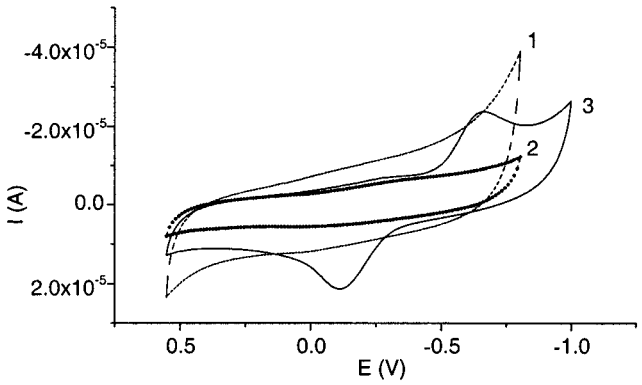

Figure 7. Cyclic voltammograms recorded in Tris 0.1 M/$HClO_4$ of pH 7.0, using (1) bare GCE and (2, 3) modified with HYDPt-1 layer, (2) prior and (1, 3) following adsorption of azobenzene. Time of self-assembly in the solution containing 1 mg azobenzene/1 mL methanol: 20 min. Scan rate 0.1 V/s.

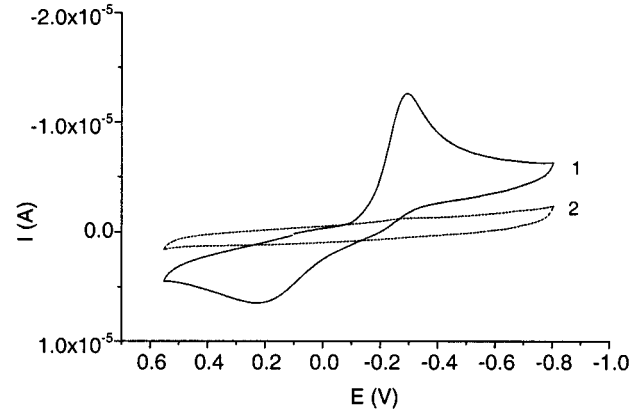

Figure 8. Cyclic voltammograms recorded in 0.1 M/$HClO_4$ of pH 7, using (1) bare GCE and (2) modified with HYDPt-1 layer, following adsorption of quinone Q0. Time of self-assembly in solution containing 1×10^{-5} M Q0 in methanol: 20min. Scan rate 0.1 V/s.

recorded in 0.1 M Tris/$HClO_4$ solution of pH 7.0. Curve 1 was recorded after adsorption of the azobenzene for the same laps of time, but on the bare GCE. The well-developed reduction and oxidation peaks do not change upon repeated cycling. The peak currents increase linearly with square root of the scan rate, indicating diffusion control rather than surface-immobilized species. Since the working solution does not contain azobenzene, this dependence can be understood in terms of diffusion of azobenzene within the HYDPt-1 layer. Such behavior argues that, in the self-assembly process, the small and hydrophobic azobenzene molecule penetrates into and is immobilized in the HYDPt-1 layer. The azobenzene incorporated into the film is now being studied in our laboratories as a molecular switching device, based on the cis−trans isomerization taking place on UV irradiation. Similar scan rate dependencies were observed for the Q0 molecule, which has the same headgroup as Q10 but does not possess an alkyl chain (Figure 8), and therefore can easily penetrate the HYDPt-1 layer.

Conclusions

The results above demonstrate for the first time that a small fungal protein, hydrophobin HYDPt-1, can be used to modify different hydrophilic and hydrophobic electrode surfaces by self-assembly from aqueous solutions, and that HYDPt-1 can act either as a molecular glue or as a matrix for electroactive molecules, depending on their structure. While the time of self-assembly of HYDPt-1 is shorter with the TMFE than with GCE and GE (respectively, 20 min and 24 h), the coverage of the surface is much higher with the hydrophobic GCE and TMFE than with the hydrophilic GE. The adsorbed HYDPt-1 layers are stable for several weeks on all types of electrodes used in solutions of a wide range of pH, blocking both the oxidation of electrode substrates, and the access of small hydrophilic electroactive probes to the electrode surface. Thus the present approach paves the way to elaborate new functional surfaces.

Acknowledgment. This work was supported by Polonium Grant for the French-Polish cooperation N° 01796NM − (120-501/67-UM992/2). We thank Dr. J. F. Kenney for revising the English.

Note Added after ASAP Posting

This article was released ASAP on 8/7/2001 with an error in a genus name. This correct version was posted on 9/7/2001.

References and Notes

(1) Finklea, H. O. Electrochemistry of Organized Monolayers of Thiols and Related Molecules on Electrodes. In *Electroanalytical Chemistry*; Bard, A. J., Rubinstein, I., Eds.; Marcel Dekker: New York, 1996; Vol. 139, pp 109−235.

(2) Herr, B. R.; Mirkin, C. A. *J. Am. Chem. Soc.* **1994**, *116*, 1157−1158.

(3) Caldwell, W. B.; Campbell, D. J.; Chen, K.; Herr, B R.; Mirkin, C. A.; Malik, K.; Durbin, M. K.; Dutta, P.; Huang, K. G. *J. Am. Chem. Soc.* **1995**, *117*, 6071−6082.

(4) Zak, J.; Yuan, H.; Ho, M.; Woo, L. K.; Porter, M. D. *Langmuir* **1993**, *9*, 2772−2774.

(5) Chidsey, C. E. D.; Bertozzi, C. R.; Putvinski, T. M.; Mujsce, A. M. *J. Am. Chem. Soc.* **1990**, *112*, 4301−4306.

(6) Wessels, J. G. H. *Trends. Plant Sci.* **1996**, *1*, 9−15.

(7) Wessels, J. G. H. *Adv. Microb. Physiol.* **1997**, *38*, 1−45.

(8) Wösten, H. A. B.; Richter, M.; Willey, J. M. *Fungal Genet. Biol.* **1999**, *27*, 153−160.

(9) Wösten, H. A. B.; de Vocht, M. L. *Biochim. Biophys. Acta* **2000**, *1469*, 79−86.

(10) Wösten, H. A. B.; van Wetter, M.-A.; Lugones, L. G.; van der Mei, H. C.; Busscher, H. J.; Wessels, J. G. H. *Curr. Biol.* **1999**, *9*, 85−88.

(11) Wessels, J. G. H. *Fungal Genet. Biol.* **1999**, *27*, 134−145.

(12) Talbot, N. J. *Nature* **1999**, *398*, 295−296.

(13) Wösten, H. A. B.; Schuren, F. H. J.; Wessels, J. G. H. *EMBO J.* **1994**, *13*, 5848−5854.

(14) Tagu, D.; Nasse, B.; Martin, F. *Gene* **1996**, *168*, 93−97.

(15) de Vocht, M. L.; Reviakine, I.; Wösten, H. A. B.; Brisson, A.; Wessels, J. G. H.; Robillard, G. T. *J. Biol. Chem.* **2000**, *275*, 28428−28432.

(16) de Vries, O. M. H.; Fekkes, M. P.; Wösten, H. A. B.; Wessels, J. G. H. *Arch. Microbiol.* **1993**, *159*, 330−335.

(17) van der Vegt, W.; van der Mei, H. C.; Wösten, H. A. B.; Wessels, J. G. H.; Busscher, H. J. *Biophys. Chem.* **1996**, *57*, 253−260.

(18) Wösten, H. A. B.; de Vries, O. M. H.; Wessels, J. G. H. *Plant Cell* **1993**, 5, 1567−1574.

(19) Wösten, H. A. B.; Ruardy, T. G.; van der Mei, H. C.; Busscher, H. J.; Wessels, J. G. H. *Colloids Surf. B: Biointerfaces* **1995**, *5*, 189−194.

(20) Wösten, H. A. B.; de Vries., O. M. H.; van der Mei, H. C.; Busscher, H. J.; Wessels, J. G. H. *J. Bacteriol.* **1994**, *176*, 7085−7086.

(21) Gunning, A. P.; De Groot, P. W. J.; Visser, J.; Morris V. J. *J. Colloid Interface Sci.* **1998**, *201*, 118−126.

(22) de Vocht, M. L.; Scholtmeijer, K.; van der Vegte, E. W.; de Vries, O. M. H.; Sonveaux, N.; Wösten, H. A. B.; Ruysschaert, J.-M.; Hadziioannou, G.; Wessels, J. G. H.; Robillard, G. T. *Biophys. J.* **1998**, 74, 2059−2068.

(23) Tagu, D.; De Bellis, R.; Balestrini, R.; de Vries, O. M. H.; Piccoli, G.; Stocchi, V.; Bonfante, P.; Martin, F. *New Phytol.* **2001**, *149*, 127−135.

(24) Rogalska, E.; Bilewicz, R.; Brigaud, T.; El Moujahid, C.; Foulard, G.; Portella, C.; Stébé, M. J. *Chem. Phys. Lipids* **2000**, *105*, 71−91.

(25) Kissa, E. *Fluorinated Surfactants: Synthesis, Properties, Applications*; Marcel Dekker: New York, 1993.

(26) Dukhin, S. S.; Kretzschmar, G.; Miller, R. Thermodynamics and macro-kinetics of adsorption. In *Dynamics of Adsorption at Liquid Interfaces*; Möbius, D., Miller, R., Eds.; Elsevier: Amsterdam ,1995; Vol. 1, pp 30−67.

(27) Bard, A. J.; Stankovich, M. T. *J. Electroanal. Chem.* **1977**, *75*, 487−505.

(28) Amatore, C.; Savéant, J. M.; Tessier, D. *J. Electroanal. Chem.* **1983**, *147*, 39−51.

(29) Bilewicz, R.; Majda, M. *Langmuir* **1991**, *7*, 2794−2802.

(30) Bilewicz, R. *Pol. J. Chem.* **1993**, *67*, 1695−1704.

(31) *Encyclopedia of Electrochemistry of the Elements*; Bard, A. J., Ed.; Plenum Press: New York, 1979; Vol. 139, p 174.